# On the Excited States Involved in the Luminescent Probe [Ru(bpy)$_2$dppz]$^{2+}$

## Enrique R. Batista and Richard L. Martin*

*Los Alamos National Laboratory, Theoretical Division, MS B268, Los Alamos, New Mexico 87545*

*Received: February 7, 2005*

The nature of the excited states of [Ru(bpy)$_2$dppz]$^{2+}$ has been investigated using density functional theory with the hybrid functional B3LYP. The excitations were studied via linear response theory (TDDFT) and ΔSCF calculations and the solvent effects were introduced by embedding the molecule in a continuum dielectric medium. It was found that the solvent effects are critical in understanding the nature of the excitations. For the molecule in ethanol, the lowest absorption predicted by TDDFT is a dark state $^3\pi \rightarrow \pi^*$ with the electron and hole spread over the dppz ligand. Next come the excitations of $^3$MLCT between the ruthenium and the dppz and finally the $^3$MLCT excitations between the ruthenium and the bpy ligands not associated with the phenazine. Using ΔSCF calculations two low-lying excited states were identified and the geometry optimized in the presence of the continuum medium. At the optimal geometry the lowest excited state is $^3$MLCT (Ru → dppz). The $^3\pi \rightarrow \pi^*$ state is found only 0.026 eV higher.

## 1. Introduction

For the past 15 years, ruthenium complexes have been the object of considerable attention, after the discovery that they serve as very sensitive luminescent reporters of DNA in aqueous solution.[1] The ruthenium complex [Ru(bpy)$_2$dppz]$^{2+}$ (bpy = 2,2′-bipyridine; dppz = dipyrido[3,2-a:2′,3′−c]phenazine) (see Figure 1) has been shown to be a remarkable light switch for DNA:[2−4] in aqueous solutions at ambient temperature, the complex shows no photoluminescence, yet in the presence of DNA the luminescence is enhanced by a factor of more than 10$^4$. It has been suggested that the luminescence of these complexes stems from a localized metal-to-ligand charge transfer (MLCT) transition. This transition is perturbed upon binding to DNA, providing a sensitive handle for interactions with nucleic acids.[5]

The "light-switch" effect in [Ru(bpy)$_2$dppz]$^{2+}$ is attributed to hydrogen bond formation in water, which quenches the excited-state luminescence. In the bound form, the dppz ligand is intercalated into the DNA strand, shielding the phenazine from the solvent and resulting in a luminescent excited state.[6] Actually, the light-switch behavior of [Ru(bpy)$_2$dppz]$^{2+}$ does not require DNA for activation; luminescence is observed in a number of aprotic environments.[7]

A detailed description of the light-switch behavior remains elusive. One leading candidate is that the light-switch arises from the presence of two $^3$MLCT states involving the dppz ligand: a bright one, associated with the bipyridine (bpy) fragment of the dppz ligand, and a dark, nonluminescent state localized largely on the phenazine (phz). It has been suggested that the light-switch is activated in protic solvents by hydrogen bond formation at the phz nitrogen atoms, which lowers the energy of the dark state below the bright state.

The experiments of Brennaman et al.[6] support the notion of bpy-like and phz-like states associated with the dppz ligand, and they also show that the bpy-like state is photophysically similar to the $^3$MLCT state of [Ru(bpy)$_3$]$^{2+}$. Their experiment also suggests that the dark (phz) state is always lowest in energy,

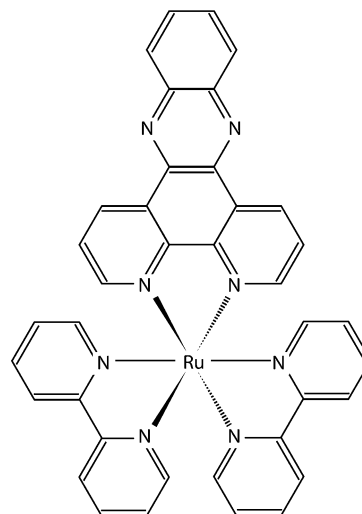**Figure 1.** [Ru(bpy)$_2$dppz]$^{2+}$ molecule.

and the light-switch behavior is governed by a competition between energetic factors that favor the dark (phz) state and entropic factors that favor the bright (bpy) state.

Despite all the experimental work on these systems, very few theoretical studies have appeared.[8,9] The most recent is from Pourtois et al.,[8] who utilize semiempirical approaches (ZINDO). This is a very effective method for mapping out excited states, and a number of their ZINDO results were corroborated with time-dependent DFT (TDDFT). However, ZINDO makes it difficult to determine reliable geometries for the luminescent states, and the role of the solvent was not addressed.

This paper presents calculations of the excitations of [Ru-(bpy)$_2$dppz]$^{2+}$ in protic and aprotic environments. The geometry of the molecule was optimized for the ground state and first excited triplet state. The excitation energies were calculated via TDDFT and ΔSCF (see section 2) including solvent effects by embedding the molecule in a polarizable dielectric continuum with the appropriate dielectric constant.

It was found that the effects of the dielectric medium are very important to the description of the excited states. The lowest

---

* Corresponding author. E-mail: rlmartin@lanl.gov

[Ru(bpy)₂dppz]²⁺ Excited States

*J. Phys. Chem. A, Vol. 109, No. 14, 2005* **3129**

state predicted by TDDFT is a $^3\pi \rightarrow \pi^*$ excitation spread over the whole dppz ligand. The bright state is assigned to a $^3$MLCT excitation. In vacuum, the lowest $^3$MLCT states transfer charge from Ru $\rightarrow$ bpy ligands not part of the dppz. In solution, we find that once the dielectric constant of the medium is greater than 4 ($\epsilon_{ethanol} = 24.55$) the ordering of the $^3$MLCT excitations changes and the lowest ones become Ru $\rightarrow$ dppz in nature. Above these follows a family of Ru $\rightarrow$ bpy excitations to the bpy ligands not incorporated within the phenazine.

If the geometry is optimized for the lowest $^3\pi \rightarrow \pi^*$ and $^3$MLCT state in solution with the $\Delta$SCF technique, then the two states are nearly degenerate with the $^3$MLCT excitation slightly lower. This can lead to a thermally activated competition between the dark and bright states as suggested by Brennaman et al.[6]

## 2. Computational Methods

The electronic structure of all the molecules presented here was determined via density functional theory (DFT) using the hybrid functional B3LYP,[10,11] which contains 25% of Hartree–Fock exchange. A double-$\zeta$ basis with polarization functions (6-31G*) was used for the ligands. The ruthenium atom was represented with the 30-electron relativistic effective core potential (RECP) LANL2, which replaces the inner shells 1 through 3 and 4s electrons, leaving explicit treatment of the 4p, 4d, and 5s electrons.[12] This RECP is the small-core potential developed from an atomic Hartree–Fock calculation, but it has been reported that these can usually be transferred to DFT calculations.[13] The basis set, LANL2DZ, was originally contracted to the results of Hartree–Fock calculations. It was completely uncontracted in order to give the basis more flexibility to adjust to the DFT potential. Uncontracted, this basis set consists of (5s5p4d). In all cases of geometry optimization, the entire molecule was fully optimized with no symmetry constraints.

The electronic excited states were calculated via density functional response theory (TDDFT),[14−17] keeping the lowest 10 singlet and 10 triplet roots for vertical excitations from the ground state. The lowest triplet states were also obtained via the difference between two separate self-consistent field calculations ($\Delta$SCF). In this methodology the solution of the Kohn–Sham equation was obtained subject to the constraint of a triplet state. This procedure yields a variational solution for the lowest triplet state, and the excitation energy is obtained as $\Delta$SCF. It also allowed us to optimize the geometry of the excited state to its minimum energy configuration, which is not currently possible to do for the TDDFT results. In some cases we were able to converge to higher lying triplet states by starting with the appropriate initial guesses for the wave function. This is possible as long as the character of the excited state is very different from the ground state (approximate orthogonality).

To model the [Ru(bpy)₂dppz]²⁺ in aprotic and protic environments, the molecule was studied in its free state and also embedded in a dielectric medium as an approximation to include solvent polarization effects. The inclusion of the dielectric medium was calculated using the IEF–PCM reaction field model.[18−20] To simulate the protic environment, two explicit water molecules were added by hydrogen bonding to the nitrogen atoms of the phenazine.
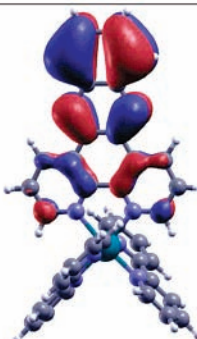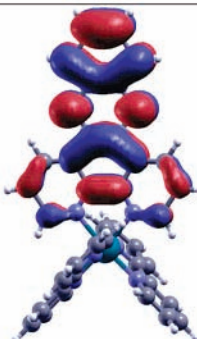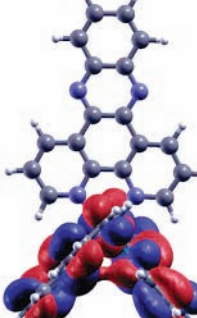
All calculations employed the GAUSSIAN03 (revision C.02)[21] suite of codes for quantum chemistry, with a local modification for the calculation of natural transition orbitals.

**TABLE 1: TDDFT Energies of the Lowest Excitations of the Free [Ru(bpy)₂dppz]²⁺ Molecule at the Optimal Geometry of the Ground State (S₀)$^a$**

| state | energy | type |
|-------|--------|------|
| S₀ | 0.00 | |
| T₁ | 2.16 | $^3\pi \rightarrow \pi^*$ |
| T₂ | 2.47 | $^3$MLCT(Ru $\rightarrow$ bpy) |
| T₃ | 2.50 | $^3$MLCT(Ru $\rightarrow$ bpy) |

$^a$ The second column shows the multiplicity of the excitation, and the last column gives the type of excitation.

**TABLE 2: NTOs of the Free Molecule**



| Exc. # | Hole | Electron | Type |
|--------|------|----------|------|
| T₁ | | | $^3\pi \rightarrow \pi^*$ |
| T₂ | | | $^3$MLCT |

## 3. Results

**3.1. Free [Ru(bpy)₂dppz]²⁺ Simulation.** The [Ru(bpy)₂dppz]²⁺ molecule in an aprotic environment was first modeled via a free molecule. The geometry of the ground-state singlet, S₀, was optimized, and vertically excited states were obtained via TDDFT calculations. The three lowest excitations are described in Table 1. A natural-transition-orbital (NTO) analysis[22,23] shows that these excitations can be described as single electron–hole pairs which reproduce over 90% of the transition density. The NTOs provide a much more compact description of the excitation in this problem, rather than looking at the molecular orbitals (MO). For example, the NTO analysis of the lowest excitation shown below is clearly a $^3\pi \rightarrow \pi^*$ excitation while the TDDFT results show it as a combination of six particle–hole pairs with transition amplitudes larger than 12%. Also, the MO that most resembles the $\pi$ orbital from where the electron is excited is the HOMO-3, showing that the relaxation of the orbitals in the excited state is significant and that the HOMO–LUMO gap is not enough to gauge the excitation energy.

The electron–hole pairs for the lowest two excitations are shown in Table 2. The third state is essentially identical to the second excitation except for a 180° phase difference in the nodal properties of the electron state. That is, it involves a virtual orbital that is symmetric with respect to the nodal plane relating the two bipyridyl groups, as opposed to the antisymmetric combination appropriate for T₂. Note that the lowest excited
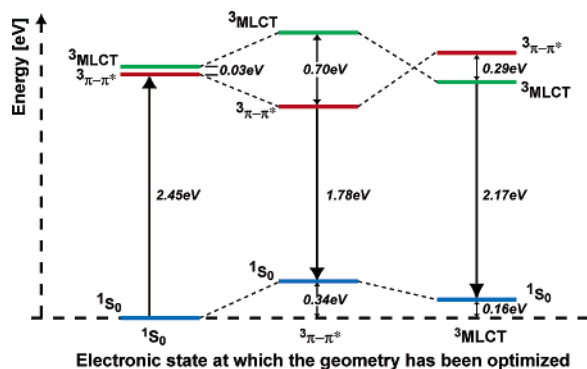
**Figure 2.** Energy landscape of the free $[Ru(bpy)_2dppz]^{2+}$ molecule. The singlet ground state $(S_0)$, $^3\pi \rightarrow \pi^*$ and $^3MLCT$ excitations are given at the optimal geometry of each state. The $^3MLCT$ state is Ru $\rightarrow$ bpy in character.

state has $^3\pi \rightarrow \pi^*$ character, with the electron−hole pair located on the dppz ligand and spread over both the phz and bpy sections. The next two triplet excitations found by TDDFT are of metal-to-ligand charge-transfer $(^3MLCT)$ type, showing a migration of $d_{x^2}$ and $d_\pi$ electrons from the Ru to a $\pi^*$ orbital on the bpy [note that if the $z$ axis is defined along the bisector of the dppz, the orbital shown in Table 2 can be characterized as $d_{x^2}$]. Here the electron transfer is to bpy groups that are not part of the dppz. These results are similar to those obtained by Pourtois et al.[8] using INDO/SCI calculations on the free [Ru-$(bpy)_2dppz]^{2+}$ molecule.

Because TDDFT assumes that the excited states can be written in terms of particle−hole excitations and hole−particle deexcitations, that is, it is a first-order theory, a more accurate description might be obtained by doing a full SCF calculation on the excited states. This also allows us to optimize their geometry. In principle, the $\Delta$SCF calculation will yield only the lowest triplet state. Due to the symmetry difference between the $^3\pi \rightarrow \pi^*$ state and the $^3MLCT$ ones, with appropriate initial guesses, two states were obtained: the $^3\pi \rightarrow \pi^*$ state and the lowest $^3MLCT$. A natural-orbital analysis of the final density shows that the unpaired electrons in the $^3\pi \rightarrow \pi^*$ state are in the dppz region with orbitals looking very much like the NTOs of the lowest TDDFT state shown in Table 2. The natural orbitals for the unpaired electrons in the $^3MLCT$ state involve a ruthenium $d_{x^2}$ orbital and a $\pi^*$ orbital in the bpy ligands not part of the dppz, as in excitation $T_2$ in Table 2. The $\Delta$SCF energy landscape for the ground state and first two excitations is shown in Figure 2. For the vertical excitation at the ground-state geometry of the molecule, the $^3\pi \rightarrow \pi^*$ is found to be only 0.03 eV lower than the $^3MLCT$ state. Upon optimization of the geometries, the $^3\pi \rightarrow \pi^*$ state remains the lowest excited state, 2.12 eV above $S_0$. The optimal $^3MLCT$ state lies 2.33 eV above $S_0$.

Additional TDDFT calculations were performed at the optimal geometry of the triplet states in order to obtain information about the entire manifold of low-lying states. The energies are shown in Table 3. The TDDFT excitation energies for the $^3MLCT$ states are in very good agreement with the $\Delta$SCF prediction for the only identifiable $^3MLCT$ state. The $^3\pi \rightarrow \pi^*$ excitation energy predicted by TDDFT is consistently 0.3 eV lower than the $\Delta$SCF prediction, even though the natural orbitals from $\Delta$SCF look identical to the NTOs from TDDFT. We do not know why this should be the case. Finally, note that the two $^3MLCT$ states are once again nearly degenerate. They involve in-phase and out-of-phase combinations of the $\pi^*$ system of bpy ligands. The near degeneracy reflects a small

**TABLE 3: TDDFT Energies of the Lowest Excitations of the Free $[Ru(bpy)_2dppz]^{2+}$ Molecule at the Optimal Geometry of the Lowest $^3\pi \rightarrow \pi^*$ State and Lowest $^3MLCT$ State[a]**

| geometry | state | energy | type |
|---|---|---|---|
| $^3\pi \rightarrow \pi^*$ | | | |
| | $T_1$ | 1.49 | $^3\pi \rightarrow \pi^*$ |
| | $T_2$ | 2.47 | $^3MLCT(Ru \rightarrow bpy)$ |
| | $T_3$ | 2.50 | $^3MLCT(Ru \rightarrow bpy)$ |
| $^3MLCT$ | | | |
| | $T_1$ | 2.16 | $^3\pi \rightarrow \pi^*$ |
| | $T_2$ | 2.20 | $^3MLCT(Ru \rightarrow bpy)$ |
| | $T_3$ | 2.20 | $^3MLCT(Ru \rightarrow bpy)$ |

[a] The second column shows the multiplicity of the excitation, and the last column gives the type of excitation. All the energies are in eV.

**TABLE 4: TDDFT Energies[a] of the Lowest 10 Excitations of the $[Ru(bpy)_2Dppz]^{2+}$ Molecule with the Nitrogen Atoms Protonated via Hydrogen Bond with Two Water, $[Ru(bpy)_2 dppz (H_2O)_2]^{2+}$**

| state | energy | type |
|---|---|---|
| $T_1$ | 2.13 | $^3\pi \rightarrow \pi^*$ |
| $T_2$ | 2.47 | $^3MLCT(Ru \rightarrow bpy)$ |
| $T_3$ | 2.50 | $^3MLCT(Ru \rightarrow bpy)$ |
| $T_4$ | 2.57 | $^3MLCT(Ru \rightarrow bpy)$ |
| $T_5$ | 2.64 | $^3MLCT(Ru \rightarrow bpy)$ |
| $S_1$ | 2.65 | $^1MLCT (Ru \rightarrow bpy)$ |
| $T_6$ | 2.65 | $^3MLCT(Ru \rightarrow dppz)$ |
| $S_2$ | 2.71 | $^1MLCT (Ru \rightarrow bpy)$ |
| $T_7$ | 2.76 | |
| $T_8$ | 2.76 | |

[a] All the energies are in eV.
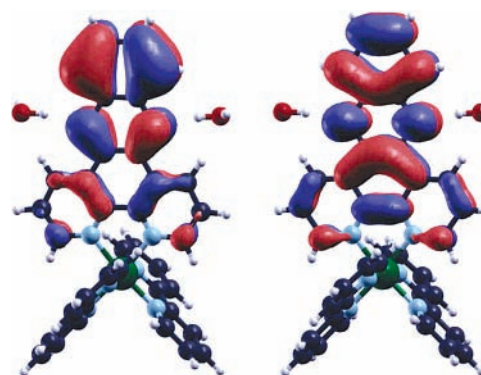


**Figure 3.** $^3\pi \rightarrow \pi^*$ excited state. Natural transition orbitals of the hole (left) and electron (right) pair.

interaction between them. They might be expected to localize quite easily in the presence of a solvent.

**3.2. $[Ru(bpy)_2dppz]^{2+}$ Molecule in Protic Environment.** The $[Ru(bpy)_2dppz]^{2+}$ molecule in a protic environment was first modeled by adding two water molecules hydrogen bonded to the nitrogen atoms, $[Ru(bpy)_2 dppz (H_2O)_2]^{2+}$. At the optimal geometry of the ground state, the water molecules form hydrogen bonds with a N−H bond distance of 1.89 Å. $H_2O$ adopts an $\eta^1$ arrangement, leaving the second hydrogen atom free to bond with solvent molecules.

The lowest 10 excitations from a TDDFT calculation are shown in Table 4. An NTO analysis of the TDDFT transition density shows that the lowest excited state is of $^3\pi \rightarrow \pi^*$ nature with the electron−hole pair localized at the dppz ligand. The NTOs are shown in Figure 3 and resemble very much the NTOs for the free molecule (see Table 2). Above the $^3\pi \rightarrow \pi^*$ excitation, between 0.34 and 0.52 eV higher, follows a set of 5 MLCT excitations. All these MLCT excitations correspond to

[Ru(bpy)$_2$dppz]$^{2+}$ Excited States

*J. Phys. Chem. A, Vol. 109, No. 14, 2005* **3131**
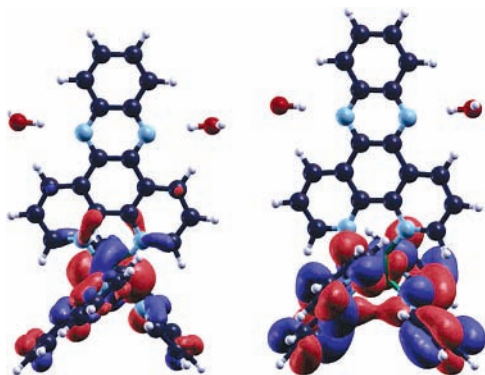


**Figure 4.** $^3$MLCT excited state. Natural transition orbitals of the hole (left) and electron (right) pair.
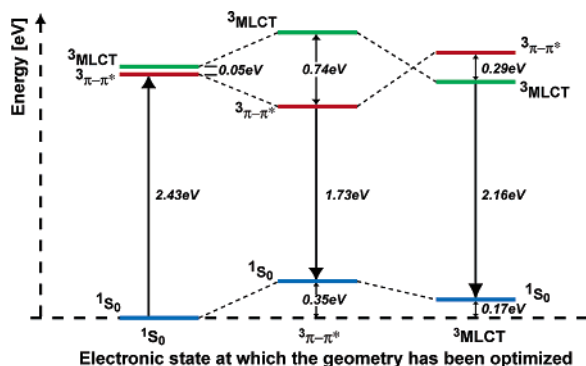


**Figure 5.** Energy levels of the [Ru(bpy)$_2$dppz]$^{2+}$ molecule with the nitrogen atoms protonated via hydrogen bond with two water, [Ru-(bpy)$_2$ dppz (H$_2$O)$_2$]$^{2+}$. The singlet ground state (S$_0$), $^3\pi \rightarrow \pi^*$ and $^3$MLCT excitations are given at the optimal geometry of each state. All the energies are given in eV. The $^3$MLCT state is Ru $\rightarrow$ bpy in character.

electrons transferred from a d$_\pi$ orbital of the Ru atom, to the bpy groups that are not connected to the phenazine. The NTOs of the electron−hole pair for the lowest $^3$MLCT excitation is shown in Figure 4. Note that the excitation energies of [Ru-(bpy)$_2$ dppz (H$_2$O)$_2$]$^{2+}$ are almost the same as those for the free molecule (see Table 1), showing that the hydrogen bonds at the nitrogen atoms of the phenazine have a minor impact in the excitations of the molecule.

As with the molecule in the aprotic environment, a full ΔSCF calculation of the energy of the lowest $^3\pi \rightarrow \pi^*$ and $^3$MLCT excited states was obtained. The energies, relative to the ground state, of the excitations of [Ru(bpy)$_2$ dppz (H$_2$O)$_2$]$^{2+}$ are shown in Figure 5. For the vertical excitations from the ground state (first column), the $^3\pi \rightarrow \pi^*$ state lies lowest, only 0.05 eV lower than the lowest $^3$MLCT state. Upon optimization of the molecular geometry for each excited state, the $^3\pi \rightarrow \pi^*$ state remains the lowest at 2.08 eV above S$_0$. The $^3$MLCT at its optimal geometry is found at 2.33 eV relative to S$_0$. A natural-orbital analysis of the open shell density shows that the NOs for the unpaired electrons of the ΔSCF calculation very much resemble the NTOs from the TDDFT calculation for the lowest two excitations.

Before leaving this theme of protic/aprotic environments, an extreme protonation limit was studied by placing a bare proton next to one of the nitrogen atoms in the phenazine and optimizing its geometry. This results in the molecule [Ru-(bpy)$_2$dppz+H]$^{3+}$. This is an extreme perturbation, and as expected, this greatly stabilizes the $\pi$ and $\pi^*$ orbitals on the dppz. The occupied $\pi$ orbital is stabilized more than the virtual $\pi^*$, and as a result, the lowest six excitations predicted by
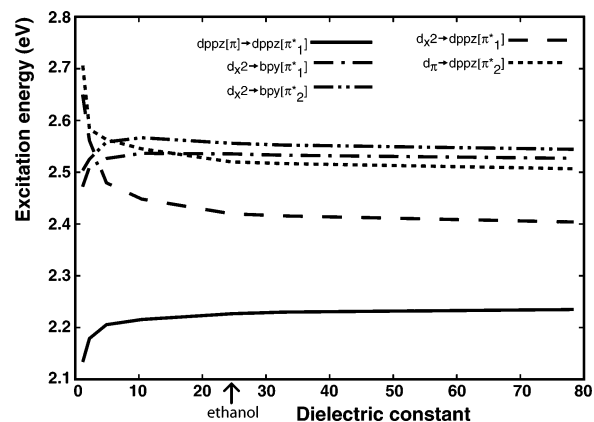


**Figure 6.** Vertical excitation energy as function of the dielectric constant of the continuum medium surrounding the molecule.

TDDFT are now of $^3$MLCT nature, where a d electron from the ruthenium is transferred to the $\pi^*$ orbital in the dppz ligand. The dppz $^3\pi \rightarrow \pi^*$ excitation now appears in seventh place, 0.48 eV higher than the lowest excited state.

## 4. Solvent Effects

The calculations presented in the previous two sections, as well as all those available in the literature,[8] have ignored the effect of the solvent on the excited states of the molecule. This section shows that those effects significantly affect the excitation energies and the nature of the excited state and cannot be ignored.

Solvent effects were modeled by surrounding the molecule with a continuum dielectric. For this, the IEF−PCM reaction field model[18−20] was used. Preliminary calculations at the gas-phase ground-state geometry were performed as function of the dielectric constant of the medium. Five excitations were identified and tracked (see Figure 6). The lowest state is always found to be the dppz-based $^3\pi \rightarrow \pi^*$ excitation, shown in Table 2. The energy of this excitation increases moderately (less than 0.1 eV) as function of the dielectric constant of the solvent. The other four excitations are of $^3$MLCT nature: The two labeled Ru[d] $\rightarrow$ bpy[$\pi^*$] are electron transfers from ruthenium Ru[d] orbitals to $\pi^*$ states in the bpy ligands not associated with the phenazine (see Table 2), and the other two, labeled Ru[d] $\rightarrow$ dppz[$\pi^*$], are electron transfers from ruthenium d orbitals to $\pi^*$ orbitals in the dppz ligand.

For the molecule in vacuum ($\epsilon = 0$), the Ru[d] $\rightarrow$ bpy[$\pi^*$] excitations discussed earlier are the second and third states, placing them lower in energy than the excitations Ru[d] $\rightarrow$ dppz-[$\pi^*$]. This quickly changes as the dielectric constant of the solvent increases past 4. A crossover is observed and, from $\epsilon = 4$ on, the second excitation becomes the $^3$MLCT from Ru to dppz. Under the experimental conditions of ref 6, which has the molecule in ethanol, the lowest excited state predicted by TDDFT is a $^3\pi \rightarrow \pi^*$ and the second and third excitations are $^3$MLCT from ruthenium to dppz.

Since the TDDFT calculations shown in Figure 6 do not contain geometric relaxation, excited state ΔSCF calculations were carried out for the [Ru(bpy)$_2$ dppz (H$_2$O)$_2$]$^{2+}$ molecule embedded in a dielectric cavity with the dielectric constant of ethanol, $\epsilon = 24.55$. The energy landscape for this situation is shown in Figure 7. As was already mentioned before, using ΔSCF calculations one can regularly obtain only one state of each symmetry or multiplicity. In the current situation two triplet states were identifiable using ad hoc initial guesses for the electronic state. The respective geometries of the excited triplet
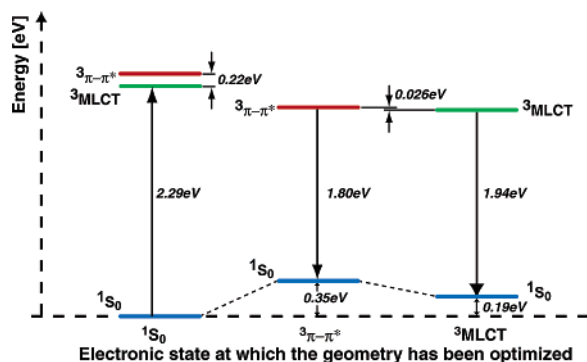
**Figure 7.** Energy landscape of the $[Ru(bpy)_2 dppz (H_2O)_2]^{2+}$ molecule embedded in a dielectric continuum medium with the dielectric constant of ethanol, $\epsilon = 24.55$. In the dielectric medium, the $^3$MLCT state is now Ru → dppz in character.

states were optimized and the $^3\pi \to \pi^*$ state was found lower in energy than the $^3$MLCT state by only 0.026 eV. At the optimal geometry of each state we could not converge to the other state. This made it impossible to know, first, how much higher the Ru[d] → bpy[$\pi^*$], lies and second, how much higher the $^3\pi \to \pi^*$ state is at the $^3$MLCT optimal geometry and vice versa.

It seems natural to associate the $^3$MLCT state with the bright state, since the spin−orbit interaction associated with the metal should break the spin selection rule. The emission energy is in good agreement with experiment; the experimental emission energy is 2.00 eV (620 nm) and the calculated one is 1.94 eV (639 nm).

It should be pointed out that a different dielectric constant should be applied to the excited and ground states to reflect the incomplete participation of the nuclear polarization component of the dielectric constant in an electronic transition. This will not influence our determination of which excited state lies lowest, as the excited state should be fully relaxed when it emits. It could affect the absolute emission energies, though. We have estimated this effect by running TDDFT with equilibration and nonequilibration of the solvent. The difference in energies obtained was on the order of $4 \times 10^{-4}$ eV, which is much smaller than the excitation energy.

## 5. Conclusions

The calculations presented in the previous sections show that, in order to understand the nature of the excited states of the $[Ru(bpy)_2dppz]^{2+}$ molecule in solution, it is crucial to include in the calculations the effect of the solvent on the electronic structure. For the molecule in the gas phase, the $^3$MLCT excited state is an electronic charge transfer from a ruthenium $d_x{}^2$ orbital to the $\pi^*$ orbital on the bpy groups that are not part of the dppz ligand ($T_2$). Once the solvent effects are included, however, it is the $^3$MLCT excitation with charge transfer to the dppz ligand ($T_6$) that is lower in energy. This stabilization of $T_6$ relative to $T_2$ in the presence of solvent could be interpreted as due to the change in dipole moment of the molecule. While the dipole moment of the molecule is not well defined because of the presence of a net charge, the relative dipole moments of the two excited states are meaningful. On one hand, in excited-state $T_2$, the transition dipole opposes the ground-state dipole moment. The molecular dipole therefore decreases with respect to the ground state, suggesting a reduction in the excitation energy in the dielectric, as observed. On the other hand, in $T_6$ charge is transferred in the opposite direction, increasing the dipole moment of the molecule and the excited-state stabilization caused by the interaction with the polarizable dielectric.

We conclude from the calculations that there exist two nearly degenerate triplet states in this molecule, one ligand based and one of MLCT character. It is natural to associate the ligand-based $^3\pi \to \pi^*$ excitation with a dark state and the $^3$MLCT(Ru → dppz[$\pi^*$]) with a bright one. This picture of nearly degenerate dark and bright states is identical to that inferred by experiment.[6,24,25] However, we suggest the dark state is of $^3\pi \to \pi^*$ nature,[25] as opposed to $^3$MLCT(Ru → bpy[$\pi^*$]).[6,24] The $\pi$ and $\pi^*$ orbitals in the dark state are located on the dppz ligand with most of the amplitude in the phenazine region. We further note that the emission energy obtained for the bright state, 1.94 eV, is in good agreement with the experimental one, 2.00 eV.

The near degeneracy of the two states is consistent with the picture presented by Brennaman et al.[6] They suggest the dark state is always lower than the bright one, but that the bright state is within thermal energy of the dark state. It is not possible to decide which of these two states lies lower from our energies alone. While we found that the bright state lies lower than the dark one by 0.026 eV, this is well within the expected error bars of the calculation. To assist experimental efforts to distinguish between the two states, we would like to estimate vibrational frequencies for them. Time-resolved Raman and infrared spectra might distinguish between the $^3\pi \to \pi^*$ excited state, in which the vibrational frequencies of the C−C bonds on the dppz ligand will be shifted, and the $^3$MLCT(Ru → bpy-[$\pi^*$]), in which the Ru−N bonds will be affected. While it is straightforward to compute the $^3\pi \to \pi^*$ frequencies, the $^3$MLCT(Ru → bpy[$\pi^*$]) state is the lowest lying triplet only in the presence of the solvent field. We cannot presently compute analytic frequencies in solution, and so this must wait for the future.

## References and Notes

(1) Jenkins, Y.; Friedman, A. E.; Turro, N. J.; Barton, J. K. *Biochemistry* **1992**, *31*, 10809.

(2) Friedman, A. E.; Chambron, J.-C.; Sauvage, J.-P.; Turro, N. J.; Barton, J. K. *J. Am. Chem. Soc.* **1990**, *112*, 4960.

(3) Friedman, A. E.; Kumar, C.; Turro, N. J.; Barton, J. K. *Nucleic Acids Res.* **1991**, *19*, 2595.

(4) Hartshorn, R. M.; Barton, J. K. *J. Am. Chem. Soc.* **1992**, *114*, 5919.

(5) Pyle, A. M.; Rehmann, J. P.; Meshoyrer, R.; Kumar, C. V.; Turro, N. J.; Barton, J. K. *J. Am. Chem. Soc.* **1989**, *111*, 2051.

(6) Brennaman, M. K.; Alstrum-Acevedo, J. H.; Fleming, C. N.; Jang, P.; Meyer, T. J.; Papanikolas, J. M. *J. Am. Chem. Soc.* **2002**, *124*, 15094.

(7) Olson, E. J. C.; Hu, D.; Hörmann, A.; Jonkman, A. M.; Arkin, M. R.; Stemp, E. D. A.; Barton, J. K.; Barbara, P. F. *J. Am. Chem. Soc.* **1997**, *119*, 11458.

(8) Pourtois, G.; Beljonne, D.; Moucheron, C.; Schumm, S.; K-De Mesmaeker, A.; Lazzaroni, R.; Brédas, J−L *J. Am. Chem. Soc.* **2004**, *126*, 683.

(9) Broo, A.; Lincoln, P. *Inorg. Chem.* **1997**, *36*, 2544.

(10) Lee, C.; Yang, W.; Parr, R. G. *Phys. Rev. B* **1988**, *37*, 785.

(11) Becke, A. D. *J. Chem. Phys.* **1993**, *98*, 5648.

(12) Hay, P. J.; Wadt, W. R. *J. Chem. Phys.* **1985** *82*, 299.

(13) Russo, T. V.; Martin, R. L.; Hay, P. J. *J. Phys. Chem.* **1995**, *99*, 17085.

(14) Jamorski, C.; Casida, M. E.; Salahub, D. R. *J. Chem. Phys.* **1996**, *104*, 5134.

(15) Petersilka, M.; Grossmann, U. J.; Gross, E. K. U. *Phys. Rev. Lett.* **1996**, *76*, 1212.

(16) Bauernschmitt, R.; Ahlrichs, R.; Hennrich, F. H.; Kappes, M. M. *J. A. Chem. Soc.* **1998** *120*, 4439.

(17) Casida, M. E. In *Recent Advances in Density Functional Methods*, Chong, D. P., Ed.; World Scientific: Singapore, 1995; Vol 1, p 391.

(18) Cancès, M. T.; Mennucci, B.; Tomasi, J. *J. Chem. Phys.* **1997**, *107*, 3032.

(19) Cossi, M.; Barone, V.; Mennucci, B.; Tomasi, J. *Chem. Phys. Lett.* **1998**, *286*, 253.

(20) Mennucci, B.; Tomasi, J. *J. Chem. Phys.* **1997**, *106*, 5151.

(21) Frisch, M. J.; Trucks, G. W.; Schlegel, H. B.; Scuseria, G. E.; Robb, M. A.; Cheeseman, J. R.; Montgomery, J. A., Jr.; Vreven, T.; Kudin, K. N.; Burant, J. C.; Millam, J. M.; Iyengar, S. S.; Tomasi, J.; Barone, V.; Mennucci, B.; Cossi, M.; Scalmani, G.; Rega, N.; Petersson, G. A.; Nakatsuji, H.; Hada, M.; Ehara, M.; Toyota, K.; Fukuda, R.; Hasegawa, J.; Ishida, M.; Nakajima, T.; Honda, Y.; Kitao, O.; Nakai, H.; Klene, M.; Li, X.; Knox, J. E.; Hratchian, H. P.; Cross, J. B.; Adamo, C.; Jaramillo, J.; Gomperts, R.; Stratmann, R. E.; Yazyev, O.; Austin, A. J.; Cammi, R.; Pomelli, C.; Ochterski, J. W.; Ayala, P. Y.; Morokuma, K.; Voth, G. A.; Salvador, P.; Dannenberg, J. J.; Zakrzewski, V. G.; Dapprich, S.; Daniels, A. D.; Strain, M. C.; Farkas, O.; Malick, D. K.; Rabuck, A. D.; Raghavachari, K.; Foresman, J. B.; Ortiz, J. V.; Cui, Q.; Baboul, A. G.; Clifford, S.; Cioslowski, J.; Stefanov, B. B.; Liu, G.; Liashenko, A.; Piskorz, P.; Komaromi, I.; Martin, R. L.; Fox, D. J.; Keith, T.; Al-Laham, M. A.; Peng, C. Y.; Nanayakkara, A.; Challacombe, M.; Gill, P. M. W.; Johnson, B.; Chen, W.; Wong, M. W.; Gonzalez, C.; Pople, J. A. *Gaussian 03*, revision C.02; Gaussian, Inc.: Pittsburgh, PA, 2003.

(22) Martin, R. L. *J. Chem. Phys.* **2003**, *118*, 4775.

(23) Batista, E. R.; Martin, R. L. Natural transition orbitals. In *Encyclopedia of Computational Chemistry*; Schleyer, P. v. R, Allinger, N. L., Clark, T., Gasteiger, J., Kollman, P. A., Schaefer, H. F., III, Schreiner, P. R., Eds.; Chichester, UK, 2004.

(24) Schoonover, J. R.; Bates, W. D.; Meyer, T. J. *Inorg. Chem.* **1995**, *34*, 6421.

(25) Önfelt, B.; Lincoln, P.; Nordén, B.; Baskin, J. S.; Zewail, Ah. H. *Proc. Natl. Acad. Sci. U.S.A.* **2000**, *97*, 5708.